

# Antiferromagnetic Structure of $\text{CrVO}_4$ and the Anhydrous Sulfates of Divalent Fe, Ni, and $\text{Co}^\dagger$

B. C. FRAZER AND P. J. BROWN  
*Brookhaven National Laboratory, Upton, New York*  
 (Received September 22, 1961)

The antiferromagnetic structures of  $\text{CrVO}_4$ ,  $\text{FeSO}_4$ ,  $\text{NiSO}_4$ , and  $\text{CoSO}_4$  have been determined from neutron diffraction data collected from polycrystalline samples. All of these compounds have the same orthorhombic crystal structure. In this structure the magnetic ions form face-centered sheets which stack at  $d_{002}$  intervals in the  $c$  direction. The magnetic structure found for  $\text{CrVO}_4$  consists of ferromagnetically ordered sheets which stack antiferromagnetically. The single spin direction is found to be inclined at angles  $\Phi_a = 27^\circ \pm 15^\circ$ ,  $\Phi_b = 64^\circ \pm 10^\circ$ , and  $\Phi_c = 81^\circ \pm 15^\circ$  with the crystallographic axes. A somewhat more logical spin orientation, which is close to being within experimental error, would be parallel to the  $a$  axis. The  $\text{Cr}^{3+}$  moment at 4.2°K is  $(2.1 \pm 0.2)\mu_B$ . The magnetic structures of  $\text{FeSO}_4$  and  $\text{NiSO}_4$  both

have antiferromagnetic sheets with ferromagnetic coupling between the sheets. In both cases the spin direction is parallel to the  $b$  axis. The moments at 4.2°K are  $(4.1 \pm 0.4)\mu_B$  for  $\text{Fe}^{2+}$ , and  $(2.1 \pm 0.1)\mu_B$  for  $\text{Ni}^{2+}$ . In  $\text{CoSO}_4$  there is also antiferromagnetic ordering within each sheet, but the coupling between sheets does not lead to a collinear spin structure. Instead there are two spin directions that alternate in successive sheets. The spin vectors are found to lie in the  $YZ$  plane at alternately clockwise and counter-clockwise angles of  $25^\circ \pm 2^\circ$  from the  $b$  axis as translations are made along the  $c$  axis. The  $\text{Co}^{2+}$  moment at 4.2°K is  $(3.3 \pm 0.2)\mu_B$ . This magnetic structure found for  $\text{CoSO}_4$  is very similar to a structure predicted recently for  $\text{CuCl}_2 \cdot 2\text{H}_2\text{O}$  by Moriya on the basis of anisotropic superexchange calculations.

## I. INTRODUCTION

CHROMIUM vanadate,  $\text{CrVO}_4$ , is a typical member of an isostructural series of orthorhombic crystals, which includes a number of anhydrous sulfates and chromates of the divalent transition elements. A recent neutron diffraction study by Frazer<sup>1</sup> and magnetic susceptibility measurements by Bozorth and Davis<sup>2</sup> have shown that  $\text{CrVO}_4$  undergoes an antiferromagnetic transition at about 50°K. It has been known for a long time that some of the sulfates have interesting magnetic properties.  $\text{FeSO}_4$ ,  $\text{MnSO}_4$ ,  $\text{NiSO}_4$ , and  $\text{CoSO}_4$  were among the first crystals examined in the pioneering low temperature magnetic measurements at the Kamerlingh Onnes Laboratory in Leiden in the early part of this century.<sup>3-5</sup> It appears that the first definite observation of a susceptibility maximum corresponding to an antiferromagnetic transition was made in the case of  $\text{FeSO}_4$ , although this was not understood at the time.<sup>3,4</sup> It may be inferred from the Leiden measurements that all of these sulfates become antiferromagnetic at low temperatures. This has been definitely established for the Fe, Ni, and Co salts in the more recent work of Borovik-Romanov, Karasik, and Kreines.<sup>6</sup> Moreover, Borovik-Romanov and Kreines<sup>7</sup> have reported that an antiferromagnetic-to-ferromagnetic transition can be induced in  $\text{CoSO}_4$  with a

field of only 12 koe. It was possible to induce the transition only along one of the crystallographic axes, and, of particular interest, the observed ferromagnetic moment was only about 30% of that to be expected from  $\text{Co}^{2+}$  ions with complete orbital quenching.

While the unusual behavior of  $\text{CoSO}_4$  is in itself sufficient to prompt neutron diffraction studies of the magnetic structures in this series, there are certain characteristics of the  $\text{CrVO}_4$  type crystal structure which also make such studies of more than routine interest. First, the orthorhombic symmetry should permit complete determination of the spin directions, and it happens that the cell dimensions in the series are favorable for this even for diffraction data from powdered crystals. Second, the crystal structure is such that the magnetic coupling must include a superexchange interaction which acts through the non-magnetic tetrahedral sulfate or vanadate groups. Neutron diffraction measurements have accordingly been undertaken to determine the magnetic structures of several of these compounds. The results obtained for  $\text{CrVO}_4$ ,  $\text{FeSO}_4$ ,  $\text{NiSO}_4$ , and  $\text{CoSO}_4$  are presented in this paper.

## II. CRYSTALLOGRAPHIC DETAILS

The crystal structure of  $\text{CrVO}_4$  was determined in an x-ray analysis by Brandt.<sup>8</sup> The positions occupied in the orthorhombic space group  $D_{2h}^{17} - Cmc$  are as follows<sup>9</sup>:

$$\begin{aligned} 4 \text{ Cr in } 4(a): & \quad (0,0,0); \\ 4 \text{ V in } 4(c): & \quad (0, y_1, \tfrac{1}{4}); \\ 8 \text{ O in } 8(f): & \quad (0, y_2, z_2); \\ 8 \text{ O in } 8(g): & \quad (x_3, y_3, \tfrac{1}{4}). \end{aligned}$$

In the structures of the anhydrous sulfates, the metal atoms occupy the 4(a) positions, the sulfur atoms the

<sup>†</sup> Work performed under the auspices of the U. S. Atomic Energy Commission.

<sup>1</sup> B. C. Frazer, *Bull. Am. Phys. Soc.* **5**, 457 (1960).

<sup>2</sup> R. M. Bozorth and D. D. Davis (private communication).

<sup>3</sup> H. Kamerlingh Onnes and A. Perrier, *Communs. Kamerlingh Onnes Lab. Univ. Leiden* **12**, 124a (1911).

<sup>4</sup> H. Kamerlingh Onnes and E. Oosterhuis, *Communs. Kamerlingh Onnes Lab. Univ. Leiden* **12**, 129b (1912) and **2**, 132e (1913).

<sup>5</sup> L. C. Jackson, *Communs. Kamerlingh Onnes Lab. Univ. Leiden* **15**, 163 (1923).

<sup>6</sup> A. S. Borovik-Romanov, V. R. Karasik, and N. M. Kreines, *Zhur. Eksp. i Teoret. Fiz.* **31**, 18 (1956) [translation: *Soviet Phys.—JETP* **4**, 109 (1957)].

<sup>7</sup> A. S. Borovik-Romanov and N. M. Kreines, *Zhur. Eksp. i Teoret. Fiz.* **35**, 1053 (1958) [translation: *Soviet Phys.—JETP* **8**, 734 (1959)].

<sup>8</sup> K. Brandt, *Arkiv Kemi* **17A**, 1 (1943).

<sup>9</sup> *International Tables for X-Ray Crystallography* (The Kynoch Press, Birmingham, England, 1952), Vol. I, p. 152.

TABLE I. Cell dimensions and parameters for  $\text{CrVO}_4$ ,  $\text{FeSO}_4$ ,  $\text{NiSO}_4$ , and  $\text{CoSO}_4$ .

	$\text{CrVO}_4^a$	$\text{FeSO}_4^b$	$\text{NiSO}_4^{c,d}$	$\text{CoSO}_4^e$
$a$	5.568 Å	5.25 Å	5.155 Å	5.195 Å
$b$	8.208 Å	7.97 Å	7.842 Å	7.872 Å
$c$	5.977 Å	6.59 Å	6.338 Å	6.523 Å
$y_1$	0.353	...	0.350	...
$y_2$	0.237	...	0.25	...
$z_2$	0.010	...	0.025	...
$x_3$	0.247	...	0.25	..
$y_3$	0.490	...	0.472	...

<sup>a</sup> See reference 8.  
<sup>b</sup> See reference 12.

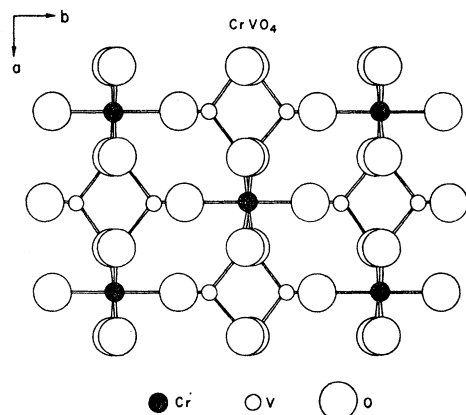
<sup>c</sup> See reference 10.  
<sup>d</sup> See reference 11.

<sup>e</sup> See reference 13.

4(c) positions, and the oxygen atoms again are found in the 8(f) and 8(g) positions. The crystal structure of  $\text{NiSO}_4$  was first determined by Dimaras<sup>10</sup> in a trial-and-error x-ray analysis and subsequently his results were confirmed, with perhaps some improvement in accuracy, by Poljak<sup>11</sup> in a Fourier series treatment of the data.  $\text{FeSO}_4$  and  $\text{CoSO}_4$  were shown to be isostructural with  $\text{CrVO}_4$  and  $\text{NiSO}_4$  by Coing-Boyat.<sup>12,13</sup>

The cell dimensions and positional parameters determined by Brandt for  $\text{CrVO}_4$  are given in Table I along with such structural details as have been determined for the sulfates. A view of the crystal structure, as seen looking down the  $c$  axis, is shown in Fig. 1. The structure consists of  $\text{MO}_6$  octahedra ( $M = \text{Cr, Fe, Ni, Co}$ ) sharing edges to form chains that propagate in the  $c$  direction, with the chains linked to one another by  $\text{VO}_4$  or  $\text{SO}_4$  tetrahedra sharing corners with the octahedra of the chains.

Since the cell dimensions of  $\text{FeSO}_4$  and  $\text{CoSO}_4$  do not differ greatly from those of  $\text{NiSO}_4$ , it may be assumed to a fairly good approximation that the sulfur and oxygen parameters are the same in all three of the sulfates, but the structure of  $\text{NiSO}_4$  was not determined

FIG. 1. The  $\text{CrVO}_4$  structure projected on (001).

<sup>10</sup> P. I. Dimaras, Acta Cryst. **10**, 313 (1957).

<sup>11</sup> R. J. Poljak, Acta Cryst. **11**, 306 (1958).

<sup>12</sup> J. Coing-Boyat, Acta Cryst. **12**, 939 (1959).

<sup>13</sup> J. Coing-Boyat, Compt. rend. **248**, 2109 (1959).

with very high accuracy. Neither can Brandt's analysis of the  $\text{CrVO}_4$  structure be considered one of high precision. As it turns out, very accurate knowledge of the crystal structures is not of critical importance to the neutron determination of the magnetic structures of these compounds. This is mostly a consequence of the simple symmetry-fixed positions of the magnetic ions. Also, most of the difficulties which result from not having very accurate positions for the nonmagnetic ions can be eliminated by subtracting neutron diffraction data collected at liquid nitrogen temperature from corresponding liquid helium data. This procedure eliminates as well whatever impurity lines that may be present. The problem of determining an accurate absolute scale factor is not eliminated, however, and of course the accuracy of the atomic moments derived from the magnetic neutron intensities depends upon the accuracy of the scale factor. As will be seen later, the  $\text{Cr}^{3+}$  moment found for  $\text{CrVO}_4$  was unexpectedly low, and it was decided to check Brandt's structure with an x-ray refinement. This work is described in Sec. IV.

### III. MAGNETIC REFERENCE DATA

Most of the magnetic measurements on these compounds have been made on polycrystalline samples. The most recent of these data are listed in Table II.  $\text{CoSO}_4$  deviates considerably from the Curie-Weiss law over a rather large temperature range above the Néel point; the susceptibility at the Néel point is almost twice the extrapolated Curie-Weiss value. Borovik-Romanov *et al.*<sup>6</sup> have offered a qualitative explanation for this behavior in terms of the splitting of the  $\text{Co}^{++}$  ground state by the crystalline field.

Single crystal magnetic measurements have been made on  $\text{CoSO}_4$  by Borovik-Romanov and Kreines.<sup>7</sup> Their most important results may be summarized as follows:

(1) Below the Néel point a ferromagnetic state can be induced with a field of only 12 koe. This occurs only for the  $a$  axis of the crystal.<sup>14</sup>

TABLE II. Magnetic properties of polycrystalline  $\text{CrVO}_4$ ,  $\text{FeSO}_4$ ,  $\text{NiSO}_4$ , and  $\text{CoSO}_4$ .

	Curie-Weiss range of validity (°K)	$C_M$	$\theta$ (°K)	$T_N$ (°K)	Effective moments <sup>d</sup> $\mu_{\text{obs}}$ ( $\mu_B$ )	$\mu_{\text{calc}}$ ( $\mu_B$ )
$\text{CrVO}_4^{a,b}$	...	...	...	~50	~4	3.87
$\text{FeSO}_4^c$	40-300	3.98	30.5	21	5.20	4.90
$\text{NiSO}_4^c$	45-300	1.83	82	37	3.82	2.83
$\text{CoSO}_4^c$	95-300	3.37	47	15.5	5.65	3.87

<sup>a</sup> See reference 1.

<sup>b</sup> See reference 2.

<sup>c</sup> See reference 6.

<sup>d</sup>  $\mu_{\text{obs}} = (3kC/N\beta^2)^{1/2}$  and  $\mu_{\text{calc}} = 2[S(S+1)]^{1/2}$ .

<sup>14</sup> The axes chosen by Borovik-Romanov and Kreines are necessarily parallel to the ones used in the present paper, but it is not certain if they are labeled in the same way.

(2) The observed ferromagnetic moment is only about 30% of that to be expected from completely quenched  $\text{Co}^{++}$  ions.

(3) The moment continued to increase slowly with the field above 12 koe, but saturation was not reached even at 18 koe.

(4) The initial susceptibility along the  $\mathbf{a}$  axis shows a very sharp anomaly at the Néel point.

(5) The susceptibility does not approach zero along any of the axes as  $T$  goes to zero.

The single-crystal measurements also indicated that the Néel point is  $12^\circ\text{K}$  instead of the value of  $15.5^\circ\text{K}$  that had been reported for a powdered specimen.

#### IV. EXPERIMENTAL

##### A. Sample Preparation

Chromium vanadate was prepared by firing  $\text{Cr}_2\text{O}_3$  with a slight excess of  $\text{V}_2\text{O}_5$  at  $750^\circ\text{C}$  for 24 hours. The sample was ground and reheated for several hours at about  $700^\circ\text{C}$ . This was done twice to assure complete reaction, and finally the sample was ground to a 300 mesh powder suitable for diffraction measurements. An x-ray diffraction pattern showed that a small amount of  $\text{Cr}_2\text{O}_3$  remained as an impurity.

The anhydrous sulfates of iron, nickel, and cobalt were prepared by heating the hydrated salts at 300, 350, and  $300^\circ\text{C}$ , respectively, for 24 hours under argon. The samples were then ground and reheated for an additional 24 hours under argon. X-ray diffraction patterns were consistent with the cell dimensions listed in Table I, and, except in the case of  $\text{FeSO}_4$ , no impurities were detected. Several additional weak lines were noted in the  $\text{FeSO}_4$  pattern which were traced to decomposition products. While these impurities did interfere to some extent with the subsequent neutron analysis, they were not of serious importance.

##### B. X-Ray Refinement of the $\text{CrVO}_4$ Structure

X-ray data were collected at room temperature on a North American Phillips diffractometer using  $\text{Cu K}\alpha$  radiation. The powdered sample was taken from the same batch used in the neutron diffraction studies. A total of 43 Bragg reflections were measured on a chart recorder and integrated with a planimeter.

Starting with Brandt's parameters for vanadium and the oxygens, the structure was refined by the method of least squares on an IBM 704 computer with the program of Busing and Levy.<sup>15</sup> Isotropic atomic temperature parameters were used in the refinement, although the data did not extend far out enough in reciprocal space to give very significant values for these parameters. No information on the atomic thermal vibrations was reported by Brandt. The final  $R$  factor obtained was 0.066 (zeros omitted), and the final

TABLE III. Comparison of  $\text{CrVO}_4$  parameters.

	Brandt <sup>a</sup>	Frazer and Brown
$y_1$	$0.353 \pm 0.005$	$0.355 \pm 0.002$
$y_2$	$0.237 \pm 0.005$	$0.241 \pm 0.003$
$z_2$	$0.010 \pm 0.005$	$0.026 \pm 0.005$
$x_3$	$0.247 \pm 0.005$	$0.251 \pm 0.004$
$y_3$	$0.490 \pm 0.005$	$0.475 \pm 0.003$
$B_{\text{Cr}}$	...	$(0.2 \pm 0.4) \text{ \AA}^2$
$B_{\text{V}}$	...	$(1.0 \pm 0.3) \text{ \AA}^2$
$B_{\text{O},f}$	...	$(1.7 \pm 0.9) \text{ \AA}^2$
$B_{\text{O},g}$	...	$(2.9 \pm 1.0) \text{ \AA}^2$

<sup>a</sup> See reference 8.

weighted  $R$  factor was 0.052 (zeros included). The resulting parameters are compared with those of Brandt in Table III, and the observed and calculated structure factors are listed in Table IV. In Table III, as in Table I, the parameter subscripts 1, 2, and 3 refer to vanadium, oxygen on the  $f$  sites, and oxygen on the  $g$  sites, respectively. The  $B$ 's are the atomic temperature parameters.

While there are some noticeable differences in the parameters obtained here and those of Brandt, particularly for  $z_2$  and  $y_3$ , the agreement is generally quite good. Nevertheless, the x-ray analysis did serve its purpose in establishing confidence in the atomic positions, and eliminating the scale error as a possible explanation of the low  $\text{Cr}^{3+}$  moment.

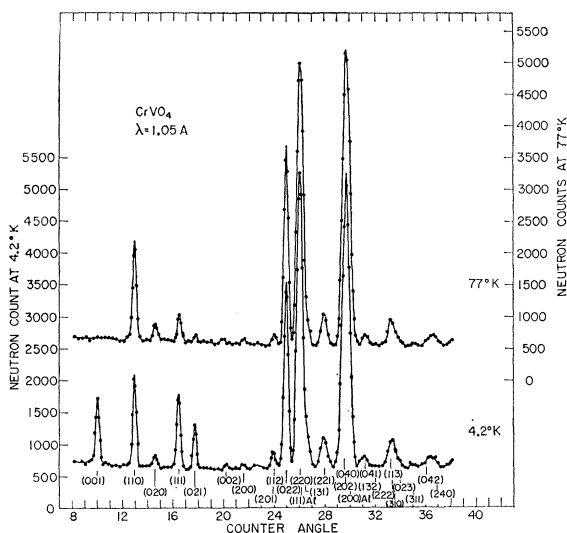
##### C. Neutron Diffraction Data

Neutron diffraction patterns were obtained from cylindrical samples of the powdered materials at liquid helium and room temperatures. In the case of  $\text{CrVO}_4$ , data were also taken at the temperature of liquid

TABLE IV. Observed and calculated x-ray structure factors for  $\text{CrVO}_4$ .

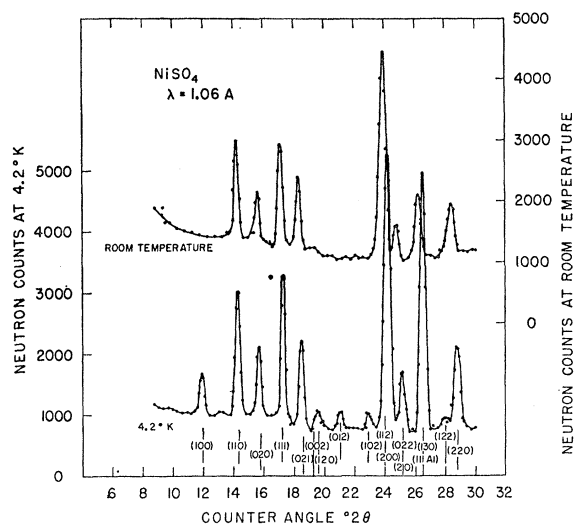
$h k l$	$ F_0 $	$F_c$	$h k l$	$ F_0 $	$F_c$
1 1 0	42	43.0	1 5 0	76	71.0
0 2 0	55	60.0	3 3 0	86	98.8
1 1 1	62	-62.9	1 5 1	44	46.0
0 2 1	86	80.4	2 2 3	42	-43.1
0 0 2	0	8.9	0 0 4	143	145.0
2 0 0	139	141	3 3 1	17	-15.2
1 1 2	116	113.2	2 4 2	132	133.1
1 3 0	128	121.9	0 4 3	27	14.2
0 2 2	0	8.9	1 1 4	24	24.2
2 2 0	27	-23.0	0 2 4	60	40.8
1 3 1	18	17.5	0 6 0	79	73.6
2 2 1	47	46.5	3 3 2	0	5.0
0 4 0	86	76.8	3 1 3	0	26.0
2 0 2	72	74.2	0 6 1	0	-19.5
0 4 1	0	-8.4	4 2 1	55	46.7
1 3 2	0	5.3	1 3 4	87	85.7
3 1 0	29	29.6	2 4 3	29	32.1
0 2 3	67	-64.8	4 0 2	0	7.7
3 1 1	47	-48.6	2 2 4	0	9.1
0 4 2	107	112.4	0 6 2	0	5.7
2 4 0	0	18.4	1 5 3	47	49.2
2 4 1	29	-38.9			

<sup>15</sup> W. R. Busing and H. Levy, Oak Ridge National Laboratory Report ORNL-59-4-37, 1959 (unpublished).

FIG. 2. Neutron diffraction patterns for  $\text{CrVO}_4$ .

nitrogen. The patterns are shown in Figs. 2-5. The work at room temperature was done primarily for scale factor determinations. In the liquid helium patterns, extra peaks appear arising from the magnetic ordering. It was found that all of the new peaks could be indexed on the original chemical unit cell. In the case of  $\text{CrVO}_4$ , some of the nuclear peaks observed at liquid nitrogen and at room temperature were found to exhibit marked increases in intensity on cooling to the temperature of liquid helium. The magnetic contributions to these peaks were determined by subtracting the liquid  $\text{N}_2$  pattern from the liquid  $\text{He}$  pattern. Such changes were not observed in the patterns of the sulfates.

The atomic positional parameters of  $\text{NiSO}_4$  were assumed for all of the sulfates in nuclear structure factor

FIG. 4. Neutron diffraction patterns for  $\text{NiSO}_4$ .

calculations. The scattering lengths used were<sup>16</sup> (in units of  $10^{-12}$  cm)

$$b_{\text{Cr}} = 0.352, \quad b_{\text{Co}} = 0.28, \quad b_{\text{Fe}} = 0.96, \quad b_{\text{Ni}} = 1.03, \\ b_{\text{V}} = -0.050, \quad b_{\text{S}} = 0.31, \quad b_{\text{O}} = 0.58.$$

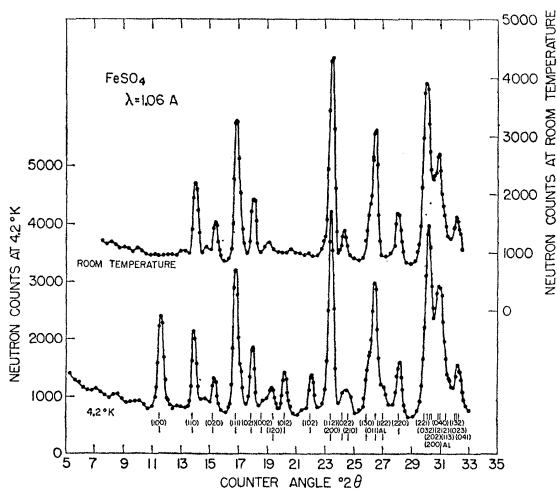
The magnetic scattering from  $\text{NiSO}_4$  was calculated using the  $\text{Ni}^{++}$  form factor found by Alperin<sup>17</sup> for  $\text{NiO}$ . The  $\text{Co}^{++}$  and  $\text{Fe}^{++}$  form factors were established by interpolation between the values for  $\text{Ni}^{++}$  and those for  $\text{Mn}^{++}$ .<sup>18</sup> The form factor assumed for  $\text{Cr}^{3+}$  was the same as that estimated for  $\text{Fe}^{++}$ . Any uncertainty in these values is probably less than the errors in the observed data.

## V. THE MAGNETIC STRUCTURES

### A. Magnetic Models

As all of the diffraction lines measured at liquid helium temperatures can be indexed in each case on the chemical cell, it must be assumed that this is also the unit cell of the magnetic structure. The four magnetic ions in this cell occupy the positions  $(0,0,0)$ ,  $(0,0,\frac{1}{2})$ ,  $(\frac{1}{2},\frac{1}{2},0)$ , and  $(\frac{1}{2},\frac{1}{2},\frac{1}{2})$ . Let the spins on each ion be represented by the vectors  $\mathbf{S}_1$ ,  $\mathbf{S}_2$ ,  $\mathbf{S}_3$ , and  $\mathbf{S}_4$ , respectively. The condition for antiferromagnetism is  $\sum \mathbf{S}_i = 0$ . In the general case there can be four spin directions in the structure. Since, for crystal chemical reasons, the spin vector magnitudes should all be equal, the angle between any two of these directions must be the same as the angle between the other two.

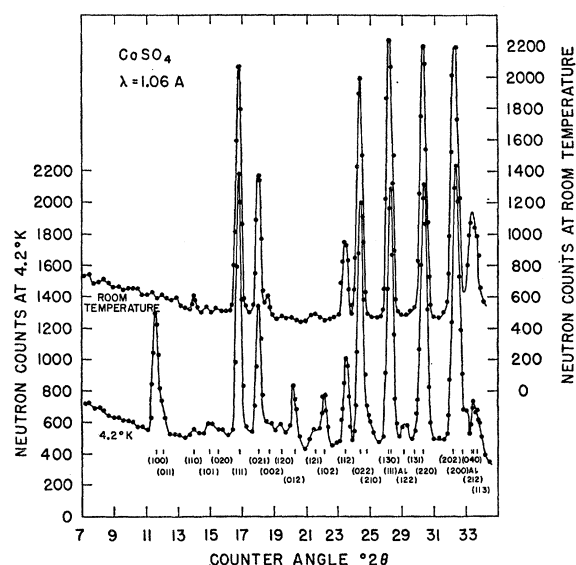
The magnetic reflection intensities for a cylindrical

FIG. 3. Neutron diffraction patterns for  $\text{FeSO}_4$ .

<sup>16</sup> C. G. Shull and E. O. Wollan, *Solid-State Physics*, edited by F. Seitz and D. Turnbull (Academic Press, Inc., New York, 1956), Vol. 2, p. 143.

<sup>17</sup> H. Alperin, *Phys. Rev. Letters* 6, 55 (1961).

<sup>18</sup> J. M. Hastings, N. Elliott, and L. M. Corliss, *Phys. Rev.* 115, 13 (1959).

FIG. 5. Neutron diffraction patterns for  $\text{CoSO}_4$ .

polycrystalline sample are given by

$$I = K j F^2 (\sin\theta \sin 2\theta)^{-1}, \quad (1)$$

where  $K$  is a scaling constant,  $j$  is the multiplicity factor,  $\theta$  is the Bragg angle, and  $F$  is the magnetic structure factor. The latter may be written in vector form as follows:

$$\mathbf{F}_{hkl} = \sum \mathbf{p}_j \mathbf{q}_j \exp[2\pi i(hx_j + ky_j + lz_j)], \quad (2)$$

where the sums extend over all magnetic ions in the unit cell,  $\mathbf{p}_j$  is the magnetic scattering amplitude, and  $\mathbf{q}_j$  is the magnetic interaction vector. Using the usual definitions of these quantities (see, for example, Bacon<sup>19</sup>), and dividing through by the constant portion of  $\mathbf{p}_j$  and the magnetic form factor, one can write a modified structure factor of the form

$$\tilde{\mathbf{F}}_{hkl} = \sum [\mathbf{e}(\mathbf{e} \cdot \mathbf{S}_j) - \mathbf{S}_j] \exp[2\pi i(hx_j + ky_j + lz_j)], \quad (3)$$

or

$$\tilde{F}_{hkl}^2 = \sum \sum [\mathbf{S}_j \cdot \mathbf{S}_k - (\mathbf{e} \cdot \mathbf{S}_j)(\mathbf{e} \cdot \mathbf{S}_k)] \times \exp\{2\pi i[h(x_j + x_k) + k(y_j + y_k) + l(z_j + z_k)]\}, \quad (4)$$

where  $\mathbf{e}$  is the unit scattering vector. This equation applies to the general case of a multi-spin axis structure, but to compare with experimental data  $\tilde{F}_{hkl}^2$  must be averaged over the sign permutations in the  $h$ ,  $k$ , and  $l$  indices.

With four spin directions in a crystal structure of the  $\text{CrVO}_4$  type, it is possible to get magnetic neutron reflections from all crystallographic planes  $(hkl)$  except those for which both  $(h+k)$  and  $l$  are even. (The latter are the only planes for which nuclear scattering by the magnetic ions is permitted.) Exami-

<sup>19</sup> G. E. Bacon, *Neutron Diffraction* (Clarendon Press, Oxford, 1955).

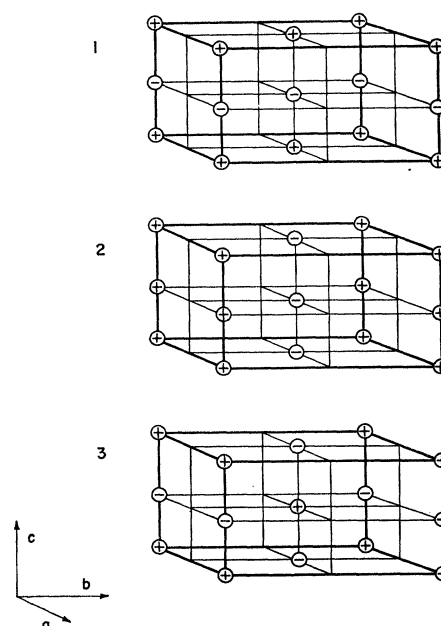


FIG. 6. The three possible antiferromagnetic collinear spin structures. The algebraic signs indicate the spin vector sense.

nation of the low-temperature neutron patterns shows that the number of magnetic lines is in each case smaller than one would expect from this general model, and suggests that the spin vectors are at least coplanar and perhaps are collinear.

The collinear case will be examined first. Clearly, the only possible antiferromagnetic structure models are the following:

$$M_1: \mathbf{S}_1 = -\mathbf{S}_2 = \mathbf{S}_3 = -\mathbf{S}_4,$$

$$M_2: \mathbf{S}_1 = \mathbf{S}_2 = -\mathbf{S}_3 = -\mathbf{S}_4,$$

$$M_3: \mathbf{S}_1 = -\mathbf{S}_2 = -\mathbf{S}_3 = \mathbf{S}_4.$$

The three collinear models are illustrated in Fig. 6. Here the only atomic positions shown are those of the magnetic ions. It is convenient to think of these structures as made up of sheets of oriented spins stacked in the  $c$  direction.  $M_1$  repeats ferromagnetic layers on  $(002)$  planes coupled antiferromagnetically;  $M_2$  has antiferromagnetic layers coupled ferromagnetically; and  $M_3$  has antiferromagnetic layers coupled antiferromagnetically.

Each model gives rise to a different set of magnetic reflections. The reflections permitted are as follows:

$$M_1: (h+k) \text{ even, } l \text{ odd,}$$

$$M_2: (h+k) \text{ odd, } l \text{ even,}$$

$$M_3: (h+k) \text{ odd, } l \text{ odd.}$$

The conditions for nuclear reflections are:  $(h0l)$  reflections only for  $h$  and  $l$  even, and  $(hkl)$  reflections only for  $(h+k)$  even. From this it can be seen that  $M_1$  gives some magnetic reflections that are from the same

planes as nuclear reflections, although there can be no nuclear contribution to these reflections from the magnetic ions. For the other two models the nuclear and magnetic reflections are different.

Examination of the neutron patterns shows that  $\text{CrVO}_4$  has an  $M_1$  structure whereas  $\text{FeSO}_4$  and  $\text{NiSO}_4$  both have  $M_2$  structures. The liquid helium pattern for  $\text{CoSO}_4$  shows magnetic reflections characteristic of both  $M_2$  and  $M_3$ , however. It is possible to account for this with a coplanar model.

If the spin vectors are coplanar the vector polygon  $\sum \mathbf{S}_j = 0$  forms a rhombus, and hence there are two spin directions. As in the collinear case, there are three possible models:

$$M_{13}: \quad \mathbf{S}_1 = -\mathbf{S}_2 \quad \mathbf{S}_3 = -\mathbf{S}_4,$$

$$M_{23}: \quad \mathbf{S}_1 = -\mathbf{S}_3 \quad \mathbf{S}_2 = -\mathbf{S}_4,$$

$$M_{12}: \quad \mathbf{S}_1 = -\mathbf{S}_4 \quad \mathbf{S}_2 = -\mathbf{S}_3.$$

The subscripts of the models  $M_{ij}$  were chosen so as to indicate relationships with the collinear models. If the spin vectors are resolved into components parallel to the rhombus diagonals, the components along one diagonal form a collinear  $M_i$  structure, and those along the other diagonal form a perpendicular collinear  $M_j$  structure. Magnetic reflections are permitted which are characteristic of both  $M_i$  and  $M_j$ . Thus,  $\text{CoSO}_4$ , giving  $M_2$  and  $M_3$  reflections in its neutron pattern, must have an  $M_{23}$  structure.

## B. Structure Analyses

All of the structures of concern here are collinear except for the coplanar  $M_{23}$  configuration in  $\text{CoSO}_4$ . But the case of  $\text{CoSO}_4$  can be reduced to two collinear structures,  $M_2$  and  $M_3$ , involving separate sets of magnetic structure factors. The diagonal spin components derived in solving these two structures can then be used to construct the proper spin vectors.

Putting in the magnetic ion coordinates and averaging over  $(hkl)$ ,  $(\bar{h}kl)$ ,  $(h\bar{k}l)$ , and  $(hkl)$ , it is possible to write Eq. (4) for collinear spins as follows:

$$F_{hkl}^2 = 16d_{hkl}^2 \left[ S_x^2 \left( \frac{k^2}{b^2} + \frac{l^2}{c^2} \right) + S_y^2 \left( \frac{h^2}{a^2} + \frac{l^2}{c^2} \right) + S_z^2 \left( \frac{h^2}{a^2} + \frac{k^2}{b^2} \right) \right], \quad (5)$$

where

$$d_{hkl}^2 = \left( \frac{h^2}{a^2} + \frac{k^2}{b^2} + \frac{l^2}{c^2} \right)^{-1},$$

and  $S_x$ ,  $S_y$ , and  $S_z$  are spin vector components in the directions of the crystallographic axes. This expression for  $\bar{F}^2$  was used in least squares analyses for the spin vector components. The magnetic intensities observed in the neutron patterns were put on an absolute scale

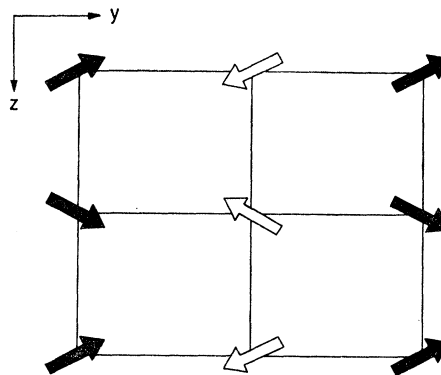


FIG. 7. The antiferromagnetic structure of  $\text{CoSO}_4$ . The black arrows are at  $x=0$ , and the white arrows at  $x=\frac{1}{2}$ . The tilt angle from the  $\mathbf{b}$  axis is  $25^\circ \pm 2^\circ$ .

using the nuclear reflections, and then processed to give an experimental set of  $\bar{F}^2$  values.

The calculations for the sulfate structures were simplified considerably as a result of the absence of the  $(010)$  reflection in all three low-temperature neutron patterns. This reflection can only be zero for an  $M_2$  structure if  $S_x = S_z = 0$ , so that the spin must be oriented along the  $\mathbf{b}$  axis. This was assumed in the calculations, although possible deviations of  $(010)$  from being identically zero were considered in computing standard errors. The  $\mathbf{b}$  axis  $M_2$  spin orientation in  $\text{CoSO}_4$  demands that  $S_y = 0$  in the  $M_3$  part of the solution, since the two diagonal spin components must be perpendicular to one another. A least squares analysis for  $S_x$  and  $S_z$  in  $M_3$  gave a negative value for  $S_x^2$ , and best agreement is, therefore, obtained by setting  $S_x = 0$  also. The  $M_3$  spin orientation in  $\text{CoSO}_4$  is then parallel to the  $\mathbf{c}$  axis. Such simplifications were not encountered in the case of  $\text{CrVO}_4$ .

The magnetic moments found at 4.2°K for the magnetic ions are as follows:

$$\text{Cr}^{3+}: (2.1 \pm 0.2)\mu_B, \quad \text{Fe}^{2+}: (4.1 \pm 0.4)\mu_B,$$

$$\text{Ni}^{2+}: (2.1 \pm 0.1)\mu_B, \quad \text{Co}^{2+}: (3.3 \pm 0.2)\mu_B.$$

The spin vector orientation angles found for  $\text{CrVO}_4$  are  $\Phi_a = 27^\circ \pm 15^\circ$ ,  $\Phi_b = 64^\circ \pm 10^\circ$ , and  $\Phi_c = 81^\circ \pm 15^\circ$ . Both  $\text{FeSO}_4$  and  $\text{NiSO}_4$  have their spin vectors oriented parallel to the  $\mathbf{b}$  axis (to an accuracy of  $2^\circ$ ). After combining the  $M_2$  and  $M_3$  results for  $\text{CoSO}_4$ , the spin vectors are found to lie in the  $YZ$  plane at alternately clockwise and counterclockwise angles of  $25^\circ \pm 2^\circ$  from the  $\mathbf{b}$  axis as translations are made along the  $\mathbf{c}$  axis. This is illustrated in Fig. 7.

The final sets of observed and calculated structure factors for all the compounds are compared in Table V.

## VI. DISCUSSION

### A. $\text{CrVO}_4$

The results obtained for  $\text{CrVO}_4$  agree within the experimental error with those reported in the pre-

liminary study of Frazer, but for the following reasons they were somewhat different from those expected: (1) the spin direction is not consistent with the crystallographic symmetry (2) the observed moment is about  $1 \mu_B$  less than the spin-only  $\text{Cr}^{3+}$  moment of  $3 \mu_B$ .

A more logical spin orientation which is not so far from being within the standard error limits would be parallel to the **a** axis. In this case the spin vectors would lie along twofold axes and be perpendicular to the *YZ* mirror planes. The standard errors given in the preceding section do not properly indicate uncertainty in the spin direction, since they were calculated on the assumption that the form factor used was without error. Actually, this form factor cannot be considered very reliable, and the **a** axis orientation is not a too unlikely one.

The possibility of the low moment being the result of an improper form factor was considered by going through several calculations with other form factors. In every case where an appreciably larger moment was obtained, however, the structure factor agreement became decidedly worse. It must be concluded that the moment is about  $2 \mu_B$ .

### B. $\text{FeSO}_4$ and $\text{NiSO}_4$

The magnetic moments found in  $\text{FeSO}_4$  and  $\text{NiSO}_4$  agree very well with those to be expected from the divalent ions with complete orbital quenching. Also, the spin orientation parallel to the **b** axis is consistent with the crystallographic symmetry. The octahedral  $\text{MO}_6$  groups each have one of their axes very nearly parallel to the **b** axis. In  $\text{NiSO}_4$ , the only one of these sulfates for which a complete structure analysis has been done, the octahedra are tilted in the *YZ* plane by about  $4.5^\circ$  from the **b** axis, with the tilt alternating in direction as one looks along the **c** axis. If the spin vectors were aligned parallel to the axes of the octahedra, the proper magnetic structure type, rather than being  $M_2$ , would be  $M_{23}$ , as observed for  $\text{CoSO}_4$ ; however, because of the small tilt angle, the  $M_3$  type reflections would be very weak. As mentioned earlier, the  $\text{NiSO}_4$  structure is not known with any high degree of accuracy, and the true tilt angle may well be somewhat smaller than  $4.5^\circ$ . A standard error of  $2^\circ$  on the spin direction was calculated for both  $\text{FeSO}_4$  and  $\text{NiSO}_4$ . Hence, it is possible that the spin vectors do follow the octahedral axes, but even if single crystals were used this would probably be difficult to detect.

### C. $\text{CoSO}_4$

One of the points of interest in beginning the study of  $\text{CoSO}_4$  was that of determining the  $\text{Co}^{++}$  moment in the antiferromagnetic phase. This was because such a low moment had been observed by Borovik-Romanov and Kreines<sup>7</sup> in the field-induced ferromagnetic phase. Also, because of the marked deviations of the suscepti-

TABLE V. Observed and calculated magnetic structure factors.

<i>h k l</i>	$ F_o $	$ F_c $	<i>h k l</i>	$ F_o $	$ F_c $
<b>CrVO<sub>4</sub></b>					
0 0 1	2.11	2.08	2 0 1	1.23	0.98
1 1 1	1.41	1.53	2 2 1	1.20	1.04
0 2 1	1.81	1.73			
<b>FeSO<sub>4</sub></b>					
0 1 0	0	0	0 1 2	2.70	3.04
1 0 0	3.94	3.95	1 0 2	3.37	3.11
1 2 0	2.12	2.04	2 1 0	2.89	2.75
<b>NiSO<sub>4</sub></b>					
0 1 0	0	0	0 1 2	1.66	1.79
1 0 0	2.14	2.24	1 0 2	1.76	1.88
1 2 0	1.61	1.18	2 1 0	1.90	1.71
<b>CoSO<sub>4</sub></b>					
0 1 0	0	0	1 2 1	1.27	1.05
1 0 0	2.68	2.96	1 0 2	2.55	2.46
0 1 1	0.81	0.88	2 1 0	1.73	2.21
1 0 1	1.08	1.02	0 3 1	1.04	0.99
1 2 0	1.78	1.58	1 2 2	1.61	1.77
0 1 2	2.24	2.38			

bility from the Curie-Weiss law above the Néel temperature, behavior which undoubtedly is related to the peculiarities of splitting of the  $\text{Co}^{++}$  levels by the crystalline field, the moment in the ordered state was of more than passing interest. As it turns out, the  $\text{Co}^{++}$  moment agrees rather well with the normal spin-only value, although it is perhaps large enough to suggest some orbital contribution. The experimental value of  $3.3 \pm 0.2 \mu_B$  was determined at  $4.2^\circ\text{K}$ , which is about  $T_N/3$  for  $\text{CoSO}_4$ , so that the extrapolated  $0^\circ\text{K}$  moment should be about  $3.4 \pm 0.2 \mu_B$ . This is two standard deviations higher than the spin-only moment of  $3 \mu_B$ . As will be discussed below, the low moment in the ferromagnetic phase must be a result of having two spin directions in the structure.

One of the results from the study of Borovik-Romanov and Kreines can be explained immediately by the magnetic structure. They found that none of the susceptibilities measured in the antiferromagnetic phase along the three crystallographic axes approached zero as  $T$  approached  $0^\circ\text{K}$ . Of course, with two spin directions, there is no  $\chi_{11}$  corresponding directly to that of a simple collinear antiferromagnet. The direction which corresponds most closely to the parallel case is along the **b** axis, and the susceptibility in this direction, while not going to zero, should be lower than the susceptibilities along the other two axes as  $0^\circ\text{K}$  is approached. As mentioned before,<sup>14</sup> there is some uncertainty as to the correspondence of the axes used here and those chosen by Borovik-Romanov and Kreines, but at least there seems to be agreement on the **b** axis. Their  $\chi_b$  is lower than the other two susceptibilities at  $0^\circ\text{K}$ .

The magnetic structure results suggest that the other two axes should be interchanged. In the first place, one would expect  $\chi_a$  to be the largest of the three susceptibilities at  $0^\circ\text{K}$ , since this is the true perpen-

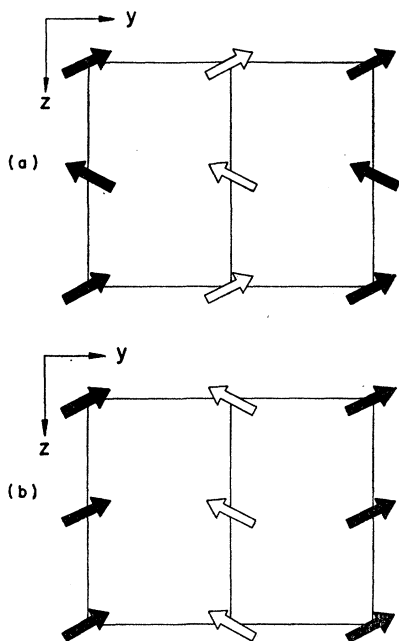


FIG. 8. Possible structures for the field-induced ferromagnetic phase of  $\text{CoSO}_4$ .

dicular susceptibility. In the Borovik-Romanov and Kreines' paper,  $\chi_c$  is the largest. The other reason for expecting this to be the case is that on examining the antiferromagnetic structure, it seems more logical to expect the field-induced ferromagnetic moment to develop in the  $c$  direction rather than along  $a$ . Two possible models for magnetization along  $c$  are shown in Fig. 8. In each model one-half of the spin vectors,  $\mathbf{S}_1$  and  $\mathbf{S}_4$ , are in the same orientations as in the antiferromagnetic structure (compare Fig. 7). In 8(a)  $\mathbf{S}_2$  and  $\mathbf{S}_3$  have been reversed, whereas in 8(b) the  $z$  components of these vectors are reversed. In either case, the effective ferromagnetic moment per cobalt ion is about  $1.4\mu_B$ , which agrees fairly well with the observation by Borovik-Romanov and Kreines of a moment of only about 30% of the spin-only  $\text{Co}^{++}$  moment. Either of these structures could also account for the continued increase in the moment with the field after the transition had been induced, since the effect of the field would be to decrease the angle between the spin vectors.

Of these two  $c$ -oriented models, 8(a) would seem to be the more likely one. In this case the crystal symmetry is obeyed and each spin vector sees the same environment. Therefore, this is the structure which is tentatively proposed here for the ferromagnetic phase. Unfortunately, a suitable magnet cryostat was not available for checking this model by neutron diffraction, but this will be possible in the near future.

The antiferromagnetic structure of  $\text{CoSO}_4$  bears some resemblance to the structure predicted recently by

Moriya<sup>20</sup> for  $\text{CuCl}_2 \cdot 2\text{H}_2\text{O}$  on the basis of an anisotropic superexchange interaction of the form  $\mathbf{D} \cdot (\mathbf{S}_i \times \mathbf{S}_j)$ . This interaction term favors a canted spin structure. No attempt has been made to carry through the complete calculations for  $\text{CoSO}_4$ , but the simple symmetry rules given by Moriya were used to find the spin vector pairs for which the antisymmetric coupling vector  $\mathbf{D}$  has a nonzero value. The only pairs that permit a nonzero value for  $\mathbf{D}$  in  $\text{CoSO}_4$  are those for which the spin vectors are noncollinear. In the case of  $\mathbf{S}_1$  and  $\mathbf{S}_2$  (or equivalently  $\mathbf{S}_3$  and  $\mathbf{S}_4$ ), where one must find the strongest coupling in the structure,  $\mathbf{D}$  is oriented parallel to the  $a$  axis.

The anisotropic superexchange theory has been applied to several cases of weak ferromagnetism, but the only antiferromagnetic example has been  $\text{CuCl}_2 \cdot 2\text{H}_2\text{O}$ . The magnetic structure of the latter has not been determined experimentally, however.  $\text{CoSO}_4$  may provide a very interesting antiferromagnetic case for applying the theory, perhaps more so than the weak ferromagnets. The local competition between ferromagnetic and antiferromagnetic interactions is certainly not trivial, since the angle between the two spin directions is about  $50^\circ$ .

#### D. Magnetic Interactions

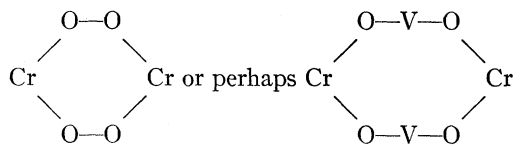
The strongest magnetic interaction is almost certainly that between  $\mathbf{S}_1$  and  $\mathbf{S}_2$  in the octahedral chains along the  $c$  axis. Assuming this to arise from superexchange, two oxygens are involved with each being in contact with both metal ions. The oxygens form the shared edge of the oxygen octahedra that surround the metal ions, and bond angles at the oxygen positions are consequently about  $90^\circ$ . The interaction is found to be antiferromagnetic for  $\text{CrVO}_4$  and ferromagnetic for  $\text{FeSO}_4$  and  $\text{NiSO}_4$ . In  $\text{CoSO}_4$  there are components of both ferromagnetic and antiferromagnetic character, with the ferromagnetic interaction predominating.

If the magnetic and chemical unit cells are identical, as proved to be the case for all of the structures reported here, then a ferromagnetic  $\mathbf{S}_1$ ,  $\mathbf{S}_2$  interaction gives a completely prescribed structure. When the interaction is antiferromagnetic, or noncollinear, the  $\mathbf{S}_1$ ,  $\mathbf{S}_3$  or the  $\mathbf{S}_1$ ,  $\mathbf{S}_4$  interaction must be fixed in order to define the magnetic structure. Each of these interactions involves superexchange along a path through the nonmagnetic tetrahedral sulfate or vanadate groups. For example, in  $\text{CrVO}_4$  the path is either  $\text{Cr}-\text{O}-\text{O}-\text{Cr}$  or perhaps as complex as  $\text{Cr}-\text{O}-\text{V}-\text{O}-\text{Cr}$ . If an examination is made of the various ways in which this linkage occurs, a single characteristic interaction is not found, and one must assume that the sign and strength of the interaction does not depend only on the type of metal ion, but on the details of interatomic distances and angles as well.

<sup>20</sup> T. Moriya, Phys. Rev. 120, 91 (1960).



Interaction between nearest equivalent magnetic ions in neighboring unit cells result from linkages of the type:



These are found to be ferromagnetic in all cases as they must be if the magnetic cell is to be identical with the chemical cell. Thus, while a single type of interaction

for a path through only one tetrahedral group does not occur, when two such paths are available, a consistent ferromagnetic interaction results.

#### ACKNOWLEDGMENTS

The authors wish to thank Dr. R. Nathans, Dr. S. J. Pickart, and Dr. F. Stern for helpful discussions of the results. They also acknowledge the valuable assistance of Mr. Ronald Horwath in the preparation of samples and associated x-ray studies.

### Reflectivity of Gray Tin Single Crystals in the Fundamental Absorption Region

MANUEL CARDONA AND D. L. GREENAWAY  
*Laboratories RCA Ltd., Zurich, Switzerland*

(Received October 2, 1961)

Single crystals of gray tin have been grown by the method of Ewald from a mercury solution. The reflection coefficient of a surface of growth has been measured in the fundamental absorption region. The reflectivity shows two maxima as in other semiconductors with diamond and zinc-blende structure. The lower energy maximum exhibits a doublet structure. The energy at which this maximum occurs is interpreted as the energy gap at the  $L$  point of the Brillouin zone. The energy separation of the doublet components gives the spin-orbit splitting of the valence band at the  $L$  point. From the measured value of the  $L$  gap the transverse effective mass at the bottom of the conduction band is estimated to be  $0.06 m$ . Several general conclusions about the systematics of the band structure in all semiconductors with diamond and zinc-blende structure are presented.

#### I. INTRODUCTION

##### A. Semiconducting Properties of Gray Tin

THE semiconducting character of gray tin was established in 1950 by several authors<sup>1</sup> from electrical measurements on polycrystalline material. Extensive studies of the galvanomagnetic properties of gray tin were performed by Busch and Wieland<sup>2</sup> and Kohnke and Ewald.<sup>3</sup> From these measurements, a value of 0.08 eV for the thermal energy gap at 0°K was obtained. The complete interpretation of these experimental results, especially the derivation of the free carrier mobilities, concentrations, and effective masses, was very difficult since conventional semiconductor techniques such as optical absorption, drift mobility, and cyclotron resonance measurements could not be applied to the polycrystalline samples available. The diamagnetic susceptibility of intrinsic and doped polycrystalline samples was studied by Busch and Moser.<sup>4</sup> By combining these measurements with the galvanomagnetic measurements and with a number of

additional assumptions, the free carrier mobilities, effective masses, and concentrations were estimated. Photoconductivity measurements on polycrystalline gray tin films were performed by Becker<sup>5</sup> at 4°K. The estimate of the energy gap obtained from these measurements (0.075 eV) is somewhat uncertain. The results of these measurements have been reviewed by Busch and Kern in a recent article.<sup>6</sup>

In 1958 Ewald and Tufte<sup>7</sup> succeeded in preparing gray tin single crystals from a saturated mercury solution at  $-30^\circ\text{C}$ . Galvanomagnetic measurements on samples from these single crystals were performed by Tufte and Ewald.<sup>8</sup> The magnetoresistance exhibited an anisotropy attributed to the electrons and corresponding to conduction-band minima along the  $[111]$  direction. The anisotropy ratio  $K$  (equal to the effective-mass anisotropy ratio divided by the scattering-time anisotropy ratio) was shown to be greater than 2.3 at room temperature. At low temperature (77°K) no magnetoresistance anisotropy was observed. This fact was attributed to the anisotropy of the ionized impurity scattering which compensates the effective mass

<sup>1</sup> A. Blum and N. A. Goryunova, *Doklady Akad. Nauk SSSR* **75**, 367 (1950); G. Busch, J. Wieland, and H. Zoller, *Helv. Phys. Acta* **23**, 528 (1950); J. T. Kendall, *Proc. Phys. Soc. (London)* **B63**, 821 (1950).

<sup>2</sup> G. Busch and J. Wieland, *Helv. Phys. Acta* **26**, 697 (1953).

<sup>3</sup> E. E. Kohnke and A. W. Ewald, *Phys. Rev.* **102**, 1481 (1956).

<sup>4</sup> G. Busch and E. Moser, *Helv. Phys. Acta* **26**, 611 (1953).

<sup>5</sup> J. H. Becker, thesis, Cornell University, 1957 (unpublished).

<sup>6</sup> G. Busch and R. Kern, *Solid-State Physics*, edited by F. Seitz and D. Turnbull (Academic Press, Inc., New York, 1960), Vol. **11**, p. 1.

<sup>7</sup> A. W. Ewald and O. N. Tufte, *J. Appl. Phys.* **29**, 1007 (1958).

<sup>8</sup> O. N. Tufte and A. W. Ewald, *Phys. Rev.* **122**, 1431 (1961).